Optical-optical double-resonance absorption spectroscopy of molecules with kHz accuracy Supporting Information

Chang-Le Hu,[†] V. I. Perevalov,[‡] Cun-Feng Cheng,[†,¶] Tian-Peng Hua,[†] An-Wen Liu,[†,¶] Yu R. Sun,[†,¶] Yan Tan,[†,¶] Jin Wang,[†,¶] and Shui-Ming Hu[*,†,¶]

† *Hefei National Laboratory for Physical Sciences at Microscale, iChem center, University of Science and Technology of China, Hefei, 230026 China*

‡*Laboratory of Theoretical Spectroscopy, V. E. Zuev Institute of Atmospheric Optics, Siberian Branch, Russian Academy of Sciences, 1, Akademician Zuev sq., 634055, Tomsk, Russia*

¶ *CAS Center for Excellence in Quantum Information and Quantum Physics, University of Science and Technology of China, Hefei, 230026 China*

E-mail: smhu@ustc.edu.cn

1. Experimental details

The configuration of the experimental setup is presented in Fig. 1. The optical cavity is composed of a pair of high-reflective (HR) mirrors ($R = 99.997\%$), with one of the mirrors mounted on a piezoelectric actuator (PZT). The mirrors are placed at two ends of a cylindrical cavity made of invar alloy. The cavity is surrounded with a heating wire controlled by a feedback servo, and the temperature was maintained at 298 K with a drift less than 10 mK in several hours. Consequently, the fractional change in cavity length is controlled to be less

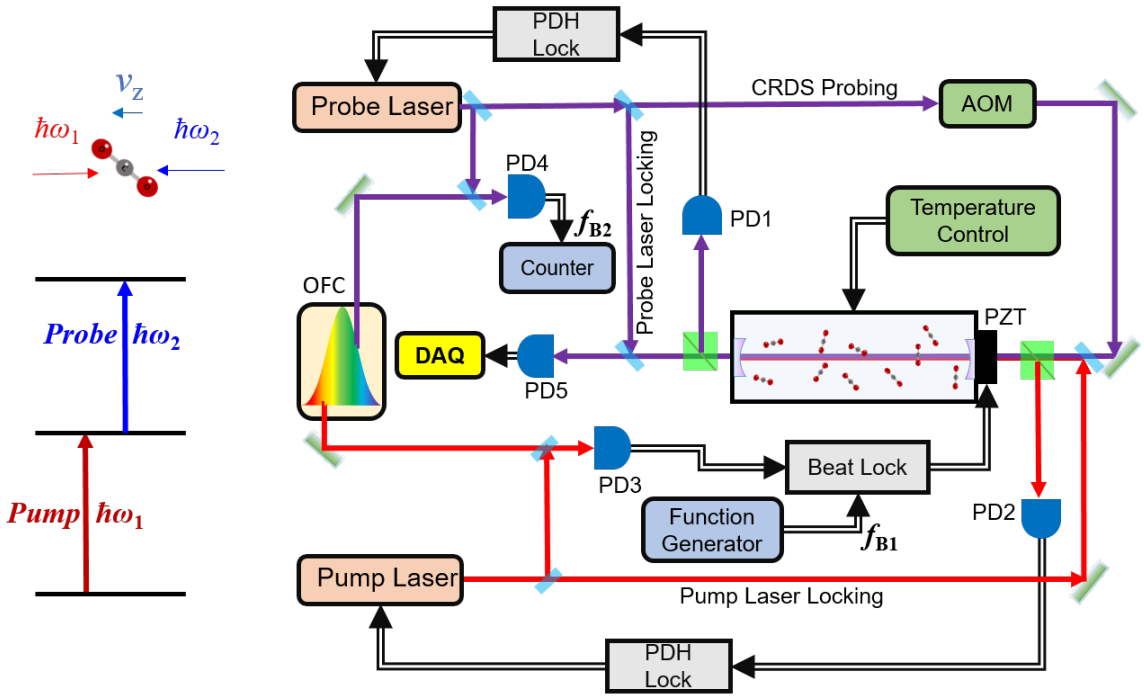

Figure 1: Configuration of the comb-locked cavity-assisted double resonance (COCA-DR) spectroscopy setup. Two lasers with frequencies denoted as ω_1 and ω_2, are locked on two cavity modes, respectively. The lasers are on resonance with molecules with a velocity of v_z, while central frequencies of the two transitions among three levels (denoted as $|\mathrm{g}\rangle$, $|\mathrm{I}\rangle$ and $|\mathrm{II}\rangle$) are ω_{10} and ω_{20} for a static molecule. Single and double lines present for laser beams and electrical lines, respectively. Abbreviations: AOM: acousto-optical modulator; DAQ: data acquisition system; OFC: optical frequency comb; PD: photodiode detector; PZT: piezoelectric actuator.

than 2×10^{-8}. The distance between two mirrors is 108 cm, leading to a free spectral range (FSR) of 139 MHz. The finesse of the cavity was determined to be 1.0×10^5 and the cavity mode width is 1.3 kHz. The whole cavity is enclosed in a stainless-steel vacuum chamber.

Two external-cavity diode lasers (Toptica DL100 Pro) were used for the pump and probe. Both lasers were locked on two respective modes of the optical cavity using the Pound-Drever-Hall (PDH) method.[1] The input power of the pump laser was about 2 mW, and the maximum power inside the cavity was estimated to be about 20 W with a beam waist radius of 0.5 mm. Probe laser light transmitted from the cavity was detected and cavity ring-down spectroscopy (CRDS) was measured. Configuration of the CRDS measurement is similar to those described in our previous studies[2–4] and will be briefly described here. The probe laser was split into two beams, one for *locking* the laser to the cavity, and the other one for *probing* the CRDS signal. The *probing* beam was frequency-shifted (and also chopped) by an acousto-optic modulator (AOM) and sent to the cavity collinearly with the *locking* beam.

Frequencies of both pump and probe lasers are calibrated by an optical frequency comb through the beating signals (f_{B1} and f_{B2} in Fig. 1). The comb is synthesized by an Er-fiber oscillator operated at 1.56 μm. The repetition frequency (f_R = 184 MHz) and the carrier offset frequency (f_0) of the comb are both referenced to a GPS-disciplined rubidium clock (SRS FS725). A feedback control servo is applied on the PZT attached to one of the HR mirrors, which stabilizes the cavity length by keeping the beat frequency equal to the frequency f_{B1} of a reference signal produced by a function generator.

Spectral scan of the DR measurement is implemented by scanning the reference frequency f_{B1}. When f_{B1} changes, the locking scheme described above changes not only the first laser frequency ω_1, but also all the cavity modes together with the second laser frequency ω_2 simultaneously. In this way, as shown in the DR scheme given in the *main text*, we are always able to reach a point satisfying the DR condition, with one laser frequency positively shifted to the first molecular line center, and the other laser frequency negatively shifted to the second transition. Here, molecules with a certain velocity v_z corresponding to the

frequency shift are selected. It is worth noting that the tuning rates of the two lasers are slightly different from each other during the scan due to the dispersion of the cavity mirrors, but the frequency of the second laser can be precisely determined by measuring its beat with the comb f_{B2}.

2. Uncertainty budget

The uncertainty budget of the transition frequency of the P(17) line in the (60025-30013) band of $^{12}C^{16}O_2$ is summarized in Table 1, and contributions from different effects are explained as follows:

(1) The statistical uncertainty derived from multiple double-resonance measurements of the P(17) line is 2.6 kHz.

(2) The line center was derived from fitting the observed spectra with a Lorentzian function. We have also tried to fit the spectra with other lineshape models, such as the Voigt profile, but did not find notable difference in line centers ($\delta\nu < 0.1$ kHz). According to the fitting residuals (an example shown in Fig. 2 of the *main text*, the asymmetry in the observed line profile should be below 1 % of the amplitude of the line. Taking into account a 140-kHz half width of the line profile, we give an estimate of 1.4 kHz as the uncertainty due to the line profile model applied in the fit.

(3) Laser frequencies were calibrated by the optical frequency comb referenced to a GPS-disciplined Rb clock (SRS FS725). The Rb clock has a stated fractional uncertainty of 2×10^{-12} at 100 s. Therefore the frequency uncertainty is 0.4 kHz at 1.6 μm.

(4) The recoil effect needs also to be considered in the double-resonance measurement. Note that the when the molecule is pumped to the intermediate state, the recoil shift is 2.9 kHz, while the recoil shift of the transition from this intermediate state is 2.8kHz with a different sign. Therefore, the overall recoil shift in this two-photon transition is -0.1kHz.

(5) The first-order Doppler shift is eliminated in present double-resonance measurements

using counter-propagating laser beams. The second-order Doppler shift is related to the velocity of the molecules. The most probable velocity of CO_2 at room temperature is 334 m/s, corresponding to a 2nd-order Doppler shift of 0.2 kHz, and the related uncertainty should be well below 0.1 kHz.

(6) The curvature of the laser wave fronts can also contribute a shift to the resonance frequency of the molecules. According to the study by Hall and Bordé,[5] the frequency shift is considerably reduced in a cavity built with high-reflective mirrors, which is estimated to be below 0.1 kHz in our experiment.

(7) Similar to the Lamb-dip measurements of the (30013-00001) band,[4] we have not observed any pressure-related shift under present experimental conditions. Collision-induced pressure shift observed in Doppler-limited studies under higher pressures ($10^3 - 10^5$ Pa) give a pressure-induced shift coefficient of 162 MHz/atm,[6] which is 0.4 kHz at a pressure of 0.25 Pa. We use this value as an estimation of the uncertainty due to possible contribution from the pressure shift.

(8) The $^{12}C^{16}O_2$ molecule has no hyperfine structure. The Zeeman splitting of the CO_2 molecule at the electronic ground state[7] is below 0.1 kHz under a magnetic field of about 0.5 Gauss.

(9) The laser power inside the cavity, although considerably enhanced by the resonance cavity, was still lower than the saturation power of the molecular transition. Typical saturation parameter was about 0.3. We measured the spectra under different laser powers, but did not observe any frequency shift within the experimental uncertainty. Similar behavior has been observed in our previous Lamb-dip studies of CO and CO_2 in the same region.[2,4] As a conservative estimation, we give an uncertainty of 1 kHz taking into account all the systematic shift due to all laser power-related effects under present experimental conditions, including the AC Stark effect and the gas-lens effect.[8]

Table 1: **Uncertainty budget for the position of the P(17) line in the (60025-30013) band of $^{12}C^{16}O_2$ (unit: kHz).**

Source	Frequency	Uncertainty
Statistical	180 220 890 030.6	2.6
Profile		1.4
Calibration		0.4
Recoil	-0.1	-
2nd-order Doppler	+0.2	< 0.1
Beam wave front		< 0.1
Collision		< 0.4
Zeeman		< 0.1
Power-related shift		1.0
Total	180 220 890 030.7	3.2

3. Transitions to the (60025) state of CO_2

A list of the energy levels obtained from the double-resonance measurement is given in Table 2. The upper energy of a rotational level in the (60025) state of $^{12}C^{16}O_2$ was derived by:

$$E'(J) = E''(J) + \hbar\omega_{01}(\mathrm{R}(J)) + \hbar\omega_{12}(\mathrm{P}(J+1)), \tag{1}$$

where $\hbar$ is the Planck constant, $E''(J)$ is the pure rotational energy with rotational angular momentum quantum number J, ω_{01} and ω_{12} are frequencies of the transition from the ground state to the intermediate state (30013) and that from the (30013) state to the upper state (60025), respectively. Rotational energies in the ground state and the transition frequencies ω_{01} were derived from Lamb-dip measurements.[4] For comparison, the calculated transition frequencies and Einstein coefficients of the lines in the (60025) - (30013) band are also given in the table. The calculation was based on the method of effective operators[9,10] . For strong transitions (with moderate J number), the experimental uncertainty is about 3 kHz and the uncertainty of derived upper energies in the (60025) state is about 5 kHz (see discussion in the *main text*).

Table 2: Energy levels of the (60025) upper state of CO_2 determined from double-resonance measurements.

	(00001)	(00001) - (30013)	P($J+1$), (30013) - (60025)			(60025)
		R(J)	P($J+1$), *exp.*	P($J+1$), *calc.*		
J	E''/h (MHz)	$\omega/2\pi$ (MHz)	$\omega/2\pi$ (MHz)	$\omega/2\pi$ (MHz)	A (s^{-1})	E'/h (MHz)
2	70 190.6760	186 777 169.0150	180 549 208.9363	180 549 788	0.215	367 396 568.6273
4	233 967.8005	186 822 067.5305	180 502 648.6129	180 503 095	0.198	367 558 683.9439
6	491 328.6863	186 866 121.1330	180 455 979.5243	180 456 222	0.189	367 813 429.3436
8	842 269.1111	186 909 327.6321	180 409 198.8285	180 409 170	0.183	368 160 795.5717
10	1 286 783.3168	186 951 684.4134	180 362 302.9921	180 361 942	0.178	368 600 770.7223
12	1 824 864.0105	186 993 188.4317	180 315 288.2779	180 314 542	0.174	369 133 340.7201
14	2 456 502.3637	187 033 836.2291	180 268 151.4009	180 266 975	0.169	369 758 489.9937
16	3 181 688.0130	187 073 623.9386	180 220 890.0306	180 219 247	0.163	370 476 201.9822
18	4 000 409.0599	187 112 547.2942	180 173 503.2950	180 171 365	0.159	371 286 459.6490
20	4 912 652.0712	187 150 601.6425	180 125 992.2471	180 123 338	0.154	372 189 245.9608
22	5 918 402.0790	187 187 781.9568	180 078 360.2423	180 075 179	0.149	373 184 544.2782
24	7 017 642.5809	187 224 082.8513	180 030 613.1890	180 026 900	0.144	374 272 338.6212
26	8 210 355.5403	187 259 498.5938	179 982 759.7987	179 978 517	0.139	375 452 613.9329
28	9 496 521.3865	187 294 023.1291	179 934 811.7414	179 930 048	0.134	376 725 356.2570
30	10 876 119.0148	187 327 650.0916	179 886 783.7984	179 881 515	0.129	378 090 552.9049
32	12 349 125.7874	187 360 372.8308	179 838 693.9018	179 832 940	0.124	379 548 192.5200
34	13 915 517.5329	187 392 184.4321	179 790 563.2815	179 784 352	0.119	381 098 265.2466
36	15 575 268.5470	187 423 077.7409	179 742 416.5409	179 735 778	0.115	382 740 762.8288
38	17 328 351.5927	187 453 045.3912	179 694 281.6778	179 687 251	0.110	384 475 678.6617
40	19 174 737.9008	187 482 079.8333	179 646 190.2963	179 638 806	0.107	386 303 008.0304
42	21 114 397.1699	187 510 173.3612	179 598 177.7787	179 590 484	0.102	388 222 748.3099
44	23 147 297.5673	187 537 318.1542	179 550 283.3524	179 542 325	0.097	390 234 899.0740
46	25 273 405.7289	187 563 506.3067	179 502 550.5064	179 494 377	0.093	392 339 462.5420
48	27 492 686.7598	187 588 729.8699	179 455 027.2833	179 446 691	0.089	394 536 443.9129
50	29 805 104.2346	187 612 980.8973	179 407 766.8063	179 399 320	0.084	396 825 851.9382
52	32 210 620.1981	187 636 251.4908	179 360 827.8690	179 352 328	0.080	399 207 699.5580
54	34 709 195.1657	187 658 533.8550	179 314 275.8275	179 305 779	0.076	401 682 004.8482
56	37 300 788.1235	187 679 820.3499	179 268 183.5781	179 259 748	0.072	404 248 792.0515
58	39 985 356.5292	187 700 103.5689	179 222 633.1223	179 214 317	0.068	406 908 093.2204
60	42 762 856.3125	187 719 376.3992	179 177 717.3350	179 169 579	0.065	409 659 950.0467
62	45 633 241.8756	187 737 632.1154	179 133 541.4162	179 125 638	0.061	412 504 415.4072
64	48 596 466.0937	187 754 864.4706	179 090 230.6371	179 082 617	0.058	415 441 561.2014
66	51 652 480.3156	187 771 067.8255	179 047 925.4591	179 040 654	0.054	418 471 473.6002
68	54 801 234.3643	187 786 237.2430	179 006 795.1841	178 999 915	0.051	421 594 266.7915
70	58 042 676.5376	187 800 368.7300	178 967 040.0357	178 960 594	0.047	424 810 085.3033

References

(1) Drever, R. W. P.; Hall, J. L.; Kowalski, F. V.; Hough, J.; Ford, G. M.; Munley, A. J.; Ward, H. Laser phase and frequency stabilization using an optical-resonator. *Appl. Phys. B* **1983**, *31*, 97–105.

(2) Wang, J.; Sun, Y. R.; Tao, L.-G.; Liu, A.-W.; Hu, S.-M. Communication: Molecular near-infrared transitions determined with sub-kHz accuracy. *J. Chem. Phys.* **2017**, *147*, 091103.

(3) Tao, L.-G.; Hua, T.-P.; Sun, Y. R.; Wang, J.; Liu, A.-W.; Hu, S.-M. Frequency metrology of the acetylene lines near 789 nm from Lamb-dip measurements. *J. Quant. Spectrosc. Radiat. Transf.* **2018**, *210*, 111.

(4) Wu, H.; Hu, C.-L.; Wang, J.; Sun, Y. R.; Tan, Y.; Liu, A.-W.; Hu, S.-M. A well-isolated vibrational state of CO_2 verified by near-infrared saturated spectroscopy with kHz accuracy. *Phys. Chem. Chem. Phys.* **2020**, *22*, 2841–2848.

(5) Hall, J. L.; Bordé, C. J. Shift and broadening of saturated absorption resonances due to curvature of the laser wave fronts. *Appl. Phys. Lett.* **1976**, *29*, 788–790.

(6) Gordon, I. E. et al. The HITRAN2016 molecular spectroscopic database. *J. Quant. Spectrosc. Radiat. Transf.* **2017**, *203*, 3–69.

(7) Kelly, M. J.; Thomas, J. E.; Monchalin, J.-P.; Kurnit, N. A.; Javan, A. Observation of Anomalous Zeeman Effect in Infrared Transitions of $^1\Sigma$ CO2 and N2O molecules. *Phys. Rev. Lett.* **1976**, *37*, 686–689.

(8) Cérez, P.; Felder, R. Gas-lens effect and cavity design of some frequency-stabilized He-Ne lasers. *Appl. Opt.* **1983**, *22*, 1251.

(9) Teffo, J.-L.; Sulakshina, O.; Perevalov, V. Effective Hamiltonian for rovibrational energies and line intensities of carbon dioxide. *J. Mol. Spectrosc.* **1992**, *156*, 48–64.

(10) Tashkun, S. A.; Perevalov, V. I.; Teffo, J.-L.; Tyuterev, V. G. Global fit of $^{12}C^{16}O_2$ vibrational-rotational line intensities using the effective operator approach. *J. Quant. Spectrosc. Radiat. Transf.* **1999**, *62*, 571–598.